HHS Public Access

Author manuscript

Eur J Neurosci. Author manuscript; available in PMC 2015 May 13.

Published in final edited form as:

Eur J Neurosci. 2011 April ; 33(8): 1504–1518. doi:10.1111/j.1460-9568.2011.07636.x.

Differential localization and function of GABA transporters, GAT-1 and GAT-3, in the rat globus pallidus

Xiao-Tao Jin, **Jean-Francois Paré**, and **Yoland Smith**

Division of Neuroscience, Yerkes National Primate Research Center and Department of Neurology, Emory University, 954 Gatewood Road NE, Atlanta, GA 30329, USA

Abstract

GABA transporter subtype 1 (GAT-1) and GABA transporter subtype 3 (GAT-3) are the main transporters that regulate inhibitory GABAergic transmission in the mammalian brain through GABA reuptake. In this study, we characterized the ultrastructural localizations and determined the respective roles of these transporters in regulating evoked inhibitory postsynaptic currents (eIPSCs) in globus pallidus (GP) neurons after striatal stimulation. In the young and adult rat GP, GAT-1 was preferentially expressed in unmyelinated axons, whereas GAT-3 was almost exclusively found in glial processes. Except for rare instances of GAT-1 localization, neither of the two transporters was significantly expressed in GABAergic terminals in the rat GP. 1-(4,4-Diphenyl-3-butenyl)-3-piperidinecarboxylic acid hydrochloride (SKF 89976A) (10 μm), a GAT-1 inhibitor, significantly prolonged the decay time, but did not affect the amplitude, of eIPSCs induced by striatal stimulation (15–20 V). On the other hand, the semi-selective GAT-3 inhibitor 1-(2-[tris(4-methoxyphenyl)methoxy]ethyl)-(*S*)-3-piperidinecarboxylic acid (SNAP 5114) (10 μM) increased the amplitude and prolonged the decay time of eIPSCs. The effects of transporter blockade on the decay time and amplitude of eIPSCs were further increased when both inhibitors were applied together. Furthermore, SKF 89976A or SNAP 5114 blockade also increased the amplitude and frequency of spontaneous IPSCs, but did not affect miniature IPSCs. Significant $GABA_A$ receptor-mediated tonic currents were induced in the presence of high concentrations of both SKF 89976A (30 μM) and SNAP 5114 (30 μM). In conclusion, these data indicate that GAT-1 and GAT-3 represent different target sites through which GABA reuptake may subserve complementary regulation of GABAergic transmission in the rat GP.

Keywords

glia; immunocytochemistry; patch-clamp recording; slice electrophysiology; striatopallidal synapse

Correspondence: Xiao-Tao Jin, as above. Jxiaota@emory.edu.

Supporting Information

Additional supporting information may be found in the online version of this article:

Fig. S1. Striatal stimulus intensity-dependent IPSCs in GP neurons.

Fig. S2. Effects of bicuculline on baseline holding current of GP neurons

Please note: As a service to our authors and readers, this journal provides supporting information supplied by the authors. Such materials are peer-reviewed and may be re-organized for online delivery, but are not copy-edited or typeset by Wiley-Blackwell. Technical support issues arising from supporting information (other than missing files) should be addressed to the authors.

Introduction

GABA is the main inhibitory neurotransmitter in the mammalian brain. After release from presynaptic terminals, GABA is rapidly removed from the extracellular space by GABA transporters (GATs), a regulatory mechanism that terminates inhibitory synaptic transmission (Borden, 1996; Richerson & Wu, 2003), regulates GABA spillover to neighboring synapses, (Borden, 1996; Overstreet & Westbrook, 2003), and maintains GABA homeostasis to prevent excessive tonic activation of synaptic and extrasynaptic GABA receptors (Borden, 1996; Semyanov *et al.*, 2004). On the other hand, reversal of GABA transport may occur during certain pathological and physiological conditions, thereby providing an additional source of GABA release (Raiteri *et al.*, 2002; Allen *et al.*, 2004; Wu *et al.*, 2007).

GAT subtype 1 (GAT-1), betaine/GABA transporter subtype 1, GAT subtype 2 (GAT-2) and GAT subtype 3 (GAT-3) are members of a large family of 12-transmembrane-spanning Na^+/Cl^--coupled transporters (Borden, 1996). Although there is compelling evidence that GAT-1 regulates GABAergic transmission in various brain regions, including the hippocampus (Thompson & Gähwiler, 1992; Isaacson *et al.*, 1993; Draguhn & Heinemann, 1996; Engel *et al.*, 1998; Overstreet *et al.*, 2000; Nusser & Mody, 2002; Overstreet & Westbrook, 2003; Semyanov *et al.*, 2003), the cerebral cortex (Keros & Hablitz, 2005; Bragina *et al.*, 2008; Gonzalez-Burgos *et al.*, 2009), the cerebellum (Rossi *et al.*, 2003), and the striatum (STR) (Kirmse *et al.*, 2008), much less is known about the role of GAT-3 in the central nervous system (CNS) (Rossi *et al.*, 2003; Galvan *et al.*, 2005; Kinney, 2005; Kirmse *et al.*, 2009). To our knowledge, only a few studies have demonstrated that GAT-1 and GAT-3 inhibitors synergistically modulate phasic and tonic $GABA_A$ conductance in the CNS (Keros & Hablitz, 2005; Kirmse *et al.*, 2009). However, GAT-3 is strongly expressed throughout the mammalian CNS (Durkin *et al.*, 1995; Minelli *et al.*, 1996; Ng *et al.*, 2000; Galvan *et al.*, 2005), suggesting a significant role in GABA regulation.

The globus pallidus (GP) (or external GP in primates) receives GABAergic inputs from the STR and from axon collaterals of GP neurons, and a major glutamatergic innervation from the subthalamic nucleus (Smith *et al.*, 1998; Plenz & Kitai, 1999; Bevan *et al.*, 2002). In turn, the GP sends GABAergic projections to the subthalamic nucleus and other basal ganglia nuclei. GAT-1 and GAT-3 are expressed in unmyelinated axons and glial processes in the monkey pallidum (Wang & Ong, 1999; Ng *et al.*, 2000; Galvan *et al.*, 2005). Although mRNA expression for both transporters has also been demonstrated in the rat GP (Durkin *et al.*, 1995; Yasumi *et al.*, 1997), the ultrastructural localization of the proteins in rodents remains unknown. We have recently demonstrated that intrapallidal application of 1-(4,4-diphenyl-3-butenyl)-3-piperidinecarboxylic acid hydrochloride (SKF 89976A), a selective GAT-1 inhibitor, or 1-(2-[tris(4-methoxyphenyl)methoxy]ethyl)-(*S*)-3-piperidinecarboxylic acid (SNAP 5114), a semi-selective GAT-3 inhibitor, reduces the firing rate of pallidal neurons in awake monkeys (Galvan *et al.*, 2005), but the synaptic mechanism(s) underlying these effects are unknown. Thus, we used electron microscopy, immunocytochemistry and whole cell patch-clamp recording techniques to provide

mechanistic insights into the regulatory functions of GATs in GABAergic striatopallidal transmission in rats.

Methods

Immunocytochemical experiments

Animals and preparation of tissue—In order to characterize the localization of GATs in rats age-matched with animals used in slice electrophysiology studies (see below), and to assess potential differences in GAT distribution patterns between these animals and adults, immunocytochemical experiments were performed in both young and adult rat brain tissue. One adult (2 months old) and two postnatal day (P)15–17 (same age range as animals used in electrophysiological experiments - see below) Sprague Dawley rats were used in the immunocytochemical experiments presented in this study. The rats were perfusion-fixed with 50–100 mL of cold, oxygenated Ringer's solution, followed by 4% paraformaldehyde and 0.1% glutaraldehyde in phosphate buffer (PB) (0.1 M, pH 7.4). Anesthesia and perfusion of the animals were perfomed in accordance with the *NIH Guide for the Care & Use of Laboratory Animals*, and were approved by Emory University's Animal Care and Use Committee. The brains were cut into 60-μm-thick sections with a vibrating microtome, and processed for the immunohistochemical localization of GAT-1 and GAT-3 at the light and electron microscopic levels, according to procedures described in detail in our previous study (Galvan *et al.*, 2005).

Pre-embedding immunoperoxidase—Sections prepared for pre-embedding immunoperoxidase were pre-treated with sodium borohydride [1% in phosphate-buffered saline (PBS); 0.01 M; pH 7.4] and then cryoprotected in a solution of 25% sucrose and 10% glycerol before being frozen at −80 °C for 20 min. They were then thawed and returned to a graded series of cryoprotectant and PBS. After this, sections were preincubated in 10% normal goat serum in PBS for 1 h, and this was followed by incubation for 48 h at 4 °C in the primary antibody solution (anti-GAT-1, 1: 500, or anti-GAT-3, 1 : 1000; Millipore, Bedford, MA, USA). The preparation and specificity tests for these antisera have been described in detail in a previous study (Ikegaki *et al.*, 1994), and they have been used extensively on rat and monkey brain tissue (Minelli *et al.*, 1995, 1996; Ribak *et al.*, 1996a,b; Conti *et al.*, 1998; Calcagnotto *et al.*, 2002; Galvan *et al.*, 2005). After three 10-min washes in PBS, the sections were incubated in biotinylated goat anti-rabbit IgG (1 : 200; Vector Laboratories, Burlingame, CA, USA) for 90 min at room temperature, and this was followed by three 10-min washes in PBS and incubation in the avidin–biotin–peroxidase complex (1 : 100; Vector Laboratories) for 90 min. After two 10-min washes in PBS and one 10-min wash in Tris buffer (0.05 M; pH 7.6), the immunostaining was revealed by incubation for 10 min in a solution containing 0.025% 3,3′-diaminobenzidine tetrahydrochloride (Sigma, St Louis, MO, USA), 0.01 M imidazole (Fisher Scientific, Atlanta, GA, USA), and 0.006% hydrogen peroxide. The reaction was stopped by repeated washes in PBS.

Preparation for light and electron microscopy—Sections used for light microscopy were processed in the same way, except that 0.1% Triton X-100 was added to the primary and secondary antibody solutions. Immunostained sections were then dehydrated, mounted

on gelatin-coated slides, and coverslipped with Permount, before being examined with a light microscope. All sections prepared for electron microscopy were washed in PB (0.1 M; pH 7.4) before being post-fixed in osmium tetroxide (1% solution in PB) for 20 min. They were then washed five times (5 min each) in PB, and dehydrated in a graded series of ethanol and propylene oxide. Uranyl acetate (1%) was added to the 70% ethanol to improve contrast in the electron microscope. The sections were then embedded in resin (Durcupan, ACM; Fluka, Buchs, Switzerland) on microscope slides, and put in the oven for 48 h at 60 °C. After examination with the light microscope, areas of interest in the GP were cut out from the slides, glued onto resin blocks, cut into ultrathin 60-nm-thick sections with a Leica (Nussloch, Germany) UCT ultramicrotome, and collected on pioloform-coated single-slot copper grids. They were then stained with lead citrate (Reynolds, 1963), and examined with a Zeiss EM-10C electron microscope.

Sampling and analysis of immunoperoxidase data—Series of 50 electron micrographs of randomly selected immunoreactive elements were taken at 31 500–43 000× from the surface of ultrathin sections cut from three blocks (two young and one adult) of GP tissue immunostained for GAT-1 or GAT-3. Together, the 150 micrographs of GAT-1-immunoreactive or GAT-3-immunoreactive structures covered a total surface of 1662 μm^2 of GP tissue. Labeled structures were categorized on the basis of ultrastructural features described in Peters *et al.* (1991). The relative percentage of a specific immunoreactive element was calculated by dividing the number of such elements by the total number of immunoreactive elements collected in each tissue block. The average percentage of each labeled structure in three rats was then calculated for GAT-1 and GAT-3.

In vitro *slice electrophysiology studies*

Slice preparation—A total of 150 young (15–17-day-old) male and female Sprague Dawley rats (Charles River Laboratories, Wilmington, MA, USA) were used in these experiments. The animals were decapitated, and the brains were removed and submerged in the ice-cold oxygenated sucrose buffer (containing 233.4 mM sucrose, 20 mM glucose, 47.3 mM $NaHCO_3$, 3 mM KCl, 1.9 mM $MgSO_4$, 1.2 mM KH_2PO_4, and 2 mM $CaCl_2$). Parasagittal or coronal (300-μm-thick) slices (four to six per animal) were made on a Vibratome 3000 (The Vibratome Company, St Louis, MO, USA) in ice-cold oxygenated sucrose buffer. The slices were stored at room temperature in a chamber containing artificial cerebrospinal fluid (ACSF) [containing 124 mM NaCl, 2.5 mM KCl, 1.3 mM $MgSO_4$, 1.0 mM NaH_2PO_4, 2.0 mM $CaCl_2$, 20 mM glucose, and 26 mM $NaHCO_3$ (pH 7.3–7.4), with 95% O_2/5% CO_2 bubbling through it; osmolarity ~310 mOsm].

Drug application—All drugs were purchased from Toris Cookson (Ellisville, MO, USA). All compounds were prepared as concentrated solutions (×1000), stored at −20 °C, and diluted in the ACSF to the appropriate concentrations immediately before bath application.

Whole cell patch clamp recording—Whole cell patch-clamp recordings were performed as described previously (Jin *et al.*, 2006; Jin & Smith, 2007). During the recording, the slice was maintained fully submerged in a recording chamber that was perfused with oxygenated ACSF (~3 mL/min). The ACSF was heated to 32–35 °C with an

in-line heater (Warner Instruments, Hamden, CT, USA), and the temperature was monitored by a thermistor placed in the recording chamber. GP neurons were visualized by IR-differential interference contrast microscopy (BX51Wl) with a × 40 water immersion objective (Olympus, Pittsburgh, PA, USA). Electrodes were pulled from borosilicate glass on a vertical patch pipette puller (Narishige, Tokyo, Japan) to have a resistance in the range of 3–5 MΩ when filled with the internal solution containing 124 mM cesium methanesulfonate, 11 mM KCl, 2 mM $MgCl_2$, 10 mM HEPES, 2 mM Na_2ATP, and 0.3 mM GTP (pH 7.4; 300–310 mOsm). QX314 (5 mM) was included to block action potential generation and postsynaptic $GABA_B$ responses (Nathan *et al.*, 1990; Andrade, 1991; McLean *et al.*, 1996).

Tight-seal (>1 GΩ) whole cell recordings were obtained from the cell bodies of GP neurons. The series resistances were regularly monitored during recording, and cells were rejected if the resistance changed by 20% or more. Neurons were voltage-clamped at a holding potential of −10 mV, and whole cell membrane currents were recorded with a Patch-Clamp PC-501A (Warner Instruments). To isolate $GABA_A$ receptor-mediated inhibitory postsynaptic currents (IPSCs), 6-cyano-7-nitroquinoxaline-2,3-dione (CNQX) (50 μM) and D-(−)-2-amino-5-phosphonopentanoic acid (D-AP5) (50 μM) were added to the ACSF.

Electrical stimulation—For striatal or pallidal stimulation, a bipolar matrix stimulating electrode (FHC, Bowdoinham, ME, USA) was placed either in the STR close to the border with the GP or in the GP itself. IPSCs in GP neurons were synaptically evoked by stimulation of either structure with single pulses that ranged from 10 to 20 V and from 150 to 200 μs, delivered once every 20 s. The failures detected by eye were excluded from all averaged responses. The baseline holding current was determined from the averaged holding current of three 200-ms epochs free of IPSCs.

Miniature IPSC (mIPSC)and spontaneous IPSC (sIPSC) recording—For recording of $GABA_A$ receptor-mediated mIPSCs and sIPSCs, the pipettes were filled with high-Cl^- electrolyte to increase the driving force of the mIPSCs and sIPSCs. The recording pipettes contained 125 mM KCl, 10 mM NaCl, 1 mM $CaCl_2$, 2 mM $MgCl_2$, 10 mM HEPES, 2 mM Na_2-ATP, 0.3 mM GTP, and 5 mM *N*-(2,6-dimethylphenylcarbamoylmethyl)-triethylammonium bromide (QX314) (pH 7.4; 300–310 mOsm). The mIPSCs were recorded at a holding potential of −60 mV in the presence of 1 μM tetrodotoxin (TTX), CNQX (50 μM), and D-AP5 (50 μM), and sIPSCs were recorded in the presence of glutamate antagonists without TTX. Data were collected continuously for 10–30 min.

Data analysis—The signals were low-pass-filtered at 5 kHz, digitized with a Digidata 1322A, and analyzed off-line with pCLAMP 9 (Molecular Devices, Union City, CA, USA). Three IPSCs were averaged, and their peak amplitude was measured before, during and after SKF 89976A or SNAP 5114 administration. In order to allow increases in amplitude to be detected, baseline recordings of IPSCs were taken at 60–80% of maximum stimulation. The decay kinetics were calculated by fitting a single exponential to the decay from ~10% below the peak. Tonic currents were calculated as the change in holding current after 7–10 min of treatment with 20 μM (+)-bicuculline (Tocris; Cat. no. 0130). The mIPSCs and sIPSCs were detected and analyzed with MINI ANALYSIS software (Synaptosoft, Fort Lee, NJ, USA).

Cumulative probability distributions were compared with Kolmogorov–Smirnov tests. All group data were expressed as means ± standard errors of the mean (SEMs). The significance of differences between groups was assessed with an unpaired Student's *t*-test.

Results

Expression of GAT-1 and GAT-3 in the GP

At the light microscopic level, moderate to strong immunoreactivity for GAT-1 and GAT-3 was found into the rat GP. Overall, the level of GAT-3 immunoreactivity in the pallidum was stronger than that for GAT-1, and significantly higher than the level of immunostaining in the adjacent STR. Most immunoreactivity for both GATs was found in the neuropil, without any specific regional pattern of distribution (Fig. 1). At high magnification, the labeling was diffuse and associated with a dense meshwork of thin processes traversing the entire extent of the GP.

At the electron microscopic level, the overall patterns of GAT-1 and GAT-3 immunoreactivity were strikingly different. GAT-1 was mainly expressed in small, unmyelinated axons, whereas GAT-3 was almost exclusively found in glial processes (Fig. 2G). In some cases, the labeled glial elements were closely apposed to axon terminals or wrapped around axo-dendritic complexes consisting of numerous unlabeled terminals and dendrites of pallidal neurons (Fig. 2A, B, E and F). The GAT-1-immunoreactive unmyelinated axons, defined as small circular (when cut transversely; Fig. 2A) or elongated (when cut longitudinally; Fig. 2D) structures containing tubular or vesicular-like processes, were commonly found in bundles piercing through the GP neuropil. Although relatively rare, GAT-1-immunoreactive terminals packed with pleomorphic electron-lucent synaptic vesicles and forming symmetrical synapses were occasionally seen (Fig. 2B and C). Neither of the two GATs was significantly expressed in postsynaptic neuronal elements. Because the patterns of distribution of GAT-1-immunoreactive and GAT-3-immunoreactive elements in young and adult rats were very similar, data collected from all rats are pooled in Fig. 2G.

Effects of GAT-1 and GAT-3 inhibitors on evoked IPSCs (eIPSCs) in the GP

Because striatal axons travel to the GP in the parasagittal plane (Kawaguchi *et al.*, 1990; Parent *et al.*, 1995), slices used for patch-clamp recordings of striatal-evoked IPSCs were cut in this plane of section to avoid significant damage to the striatopallidal pathway (see also Jin & Smith, 2007). In this slice preparation, the amplitude of eIPSCs was highly dependent on the striatal stimulus intensity. The small-amplitude IPSCs were evoked by 5-V stimulation (24.2 ± 4.9 pA, $n = 9$), whereas large-amplitude IPSCs (280 ± 39 to 331.5 ± 27 pA, $n = 9$) were evoked by 15–20-V stimulation (Supporting Information Fig. S1). In order to recruit a significant contingent of striatopallidal axons and generate strong GABAergic outflow in the GP, 15—20-V stimuli were used to activate striatofugal axons in all subsequent experiments. Because strong depolarizing stimuli could bypass action potential generation or spread to the recording sites to induce GABA release from synaptic boutons and contaminate the eIPSCs, we tested the effect of TTX (1 μM) or (+)-bicuculline (20 μM) on IPSCs evoked by 15-V striatal stimulation. Application of both TTX and bicuculline completely abolished all IPSCs (Supporting Information Fig. S1), thereby demonstrating

that the IPSCs evoked in GP neurons by strong stimulus intensities in the striatum are, indeed, action potential-dependent and mediated by $GABA_A$ receptors.

In a first series of experiments, we tested the effects of the highly specific GAT-1 blocker SKF 89976A on striatal eIPSCs. In light of *in vitro* data from hippocampal neurons showing that 10 μ_M SKF 89976A abolishes more than 75% of GAT-1-mediated IPSCs in cultured hippocampal neurons (Wu *et al.*, 2007), we used this concentration of GAT-1 blocker to test its effect on striatal eIPSCs in the GP. Bath application of SKF 89976A (10 μ_M) prolonged the decay time (148.1 ± 6.1% of control; $P = 0.002$), but had no significant effect on the amplitude (104 ± 4% of control; $P = 0.3$) or baseline holding currents (116.6 ± 12.3% of control; $P = 0.96$) of eIPSCs in six cells tested (Fig. 3A–C).

In a second set of experiments, we examined whether GAT-3 is also involved in the regulation of GABAergic transmission at striatopallidal synapses, using SNAP 5114 as a GAT-3 semi-selective antagonist (Borden, 1996). In neocortex slices, application of 20 μ_M SNAP 5114 increased the amplitude of eIPSCs and sIPSCs (Kinney, 2005). However, when used at such a high concentration, SNAP 5114 also blocks GAT-2 (Borden, 1996). Taking into consideration the IC_{50} values of SNAP 5114 for GAT-2 (~20 μ_M) and GAT-3 (5 μ_M), we applied 10 μ_M SNAP 5114 to test its effects on GABAergic synaptic transmission in the GP. At this concentration, SNAP 5114 should block more than half of the GAT-3 reuptake sites, while having minimal inhibitory effects on GAT-2. Application of 10 μ_M SNAP 5114 did, indeed, result in significant, reversible increases in both the amplitude and decay time (Fig. 3D and E) of striatal eIPSCs. In six neurons, the amplitude was 163 ± 20% of control ($P = 0.01$) and the decay time was 154 ± 14% of control ($P = 0.04$) in the presence of SNAP 5114 (Fig. 3F). The baseline holding current was not significantly different from that in controls (118.6 ± 12% of control, $P = 0.06$). These results of these experiments demonstrate that the blockade of GAT-1 or GAT-3 has profound, but partially different, regulatory effects on eIPSCs at GABAergic striatopallidal synapses in the rat GP.

Because of their substantially different patterns of distribution (Fig. 2), GAT-1 and GAT-3 may have additive effects on GABA reuptake when co-activated in the rat GP. To test this possibility, we first determined the effects of SKF 89976A (10 μ_M), alone or in combination with SNAP 5114 (10 μ_M), on eIPSCs in GP neurons after 15-V striatal stimulation. In six cells tested, application of SKF 89976A alone increased the decay time (134 ± 8% of control; $P = 0.001$), but not the amplitude (104 ± 7.7% of control; $P = 0.3$), of eIPSCs (Fig. 4A–D). However, when both SKF 89976A and SNAP 5114 were applied together, the amplitude was significantly increased to 154 ± 8.8% of control ($P = 0.001$), and the decay time of eIPSCs was further significantly enhanced to 167 ± 11.8% of control ($P = 0.001$) (Fig. 4A–D). The effects of the combined application of the two antagonists on both the amplitude and the decay time were significantly different from those observed with the application of the GAT-1 antagonist alone ($P = 0.001$) (Fig. 4D). In contrast, the holding current of eIPSCs in response to striatal stimulation was not significantly different from control in the presence of SKF 89976A alone or when combined with SNAP 5114 (123 ± 14% of control; $P = 0.07$) (Fig. 4D).

In order to determine whether the additive effects of GAT-1 and GAT-3 blockade on eIPSCs are dependent on the blockade sequence of each transporter subtype, we tested the effects of SNAP 5114 alone, or together with SKF 89976A, on eIPSCs in another five GP neurons. Application of SNAP 5114 alone increased the decay time (143 ± 11.5% of control; P = 0.001) and amplitude (150 ± 13% of control; P = 0.001) of eIPSCs (Fig. 4E–G). The decay time was further enhanced (168 ± 11.8% of control; P = 0.001) when both SNAP 5114 and SKF 89976A were applied together (Fig. 4E–G), whereas the amplitude was not significantly affected by the subsequent application of the GAT-1 antagonist (P = 0.64).

Together, these results indicate that the effects of GAT-1 and GAT-3 blockers on the decay time of striatal eIPSCs in the rat GP are partly additive, whereas only GAT-3 has any significant effect on the amplitude of eIPSCs.

Effects of GAT-1 and GAT-3 inhibitors on sIPSCs and mIPSCs

We have shown that blockade of GAT-1 and GAT-3 has profound regulatory effects on the eIPSCs at GABAergic synapses in the rat GP. To test whether these effects depend on action potential generation, we determined the regulatory functions of SKF 89976A and SNAP 5114 on sIPSCs and mIPSCs recorded in the presence or absence of 1 μ_M TTX, respectively. As shown in Fig. 5A–E, bath application of SKF 89976A (10 μ_M) increased the amplitude (128 ± 3.5% of control; P = 0.001) and frequency (136 ± 4.5% of control; P = 0.001), but not the half-decay time (102.8 ± 4.3% of control; P = 0.7), of sIPSCs in seven neurons tested in these experiments (Fig. 7A). Bath application of SNAP 5114 (10 μ_M) had similar effects on the amplitude (136 ± 6.4% of control; P = 0.001), frequency (138 ± 5.7% of control; P = 0.001) and half-decay time (115 ± 12.6% of control; P = 0.69) of sIPSCs (Figs 5F–J and 7B). As expected, combined blockade of GAT-1 and GAT-3 further increased the amplitude (173 ± 7.4% of control; P < 0.001; n = 6) and frequency (162 ± 6.1% of control; P = 0.001), without changing the half-decay time (121 ± 10% of control; P = 0.08), of sIPSCs (Fig. 7C).

In contrast to the effects on sIPSCs, bath application of SKF 89976A or SNAP 5114 alone or in combination did not alter the amplitude, frequency or half-decay time of mIPSCs in GP neurons (Figs 6 and 7D–F). Taken together, these results further demonstrate that GAT-1 and GAT-3 modulate action potential-dependent GAB-Aergic transmission in the GP.

Effects of GAT-1 and GAT-3 inhibitors on eIPSCs in coronal sections of the rat GP

Because some GP neurons project to the STR and have local axon collaterals in the GP (Kita & Kitai, 1991; Bevan *et al.*, 1998; Smith *et al.*, 1998; Kita *et al.*, 1999; Kita & Kita, 2001; Sadek *et al.*, 2007), electrical stimulation of the STR could not only orthodromically activate striatopallidal fibers, but also recruit intrinsic axon collaterals of GP neurons through antidromic activation of pallidostriatal neurons. Thus, the IPSCs evoked by striatal stimulation and sIPSCs modulated by SKF 89976A and SNAP 5114 in the previous experiments could result from activation of local axon collaterals of GP neurons, rather than striatopallidal axons. To test this possibility, we recorded IPSCs evoked by local intrapallidal stimulation in GP slices cut in the coronal plane, a section plane that maintains intrapallidal local axon collateral communication, but significantly damages the

striatopallidal pathway (Cooper & Stanford, 2001; Valenti *et al.*, 2003). Bath application of SKF 89976A or SNAP 5114 alone or in combination did not have any significant effect on either the amplitude or decay time of IPSCs evoked by 10–20-V stimulus intensities (Fig. 8A–F; $P = 0.06$; $n = 6$). The application of SKF 89976A or SNAP 5114 alone also had no significant effects on the amplitude, frequency or half-decay time of sIPSCs (Fig. 8G and H), but the combined use of both antagonists significantly increased their amplitude (139 ± 11%, $P = 0.001$) and frequency (132 ± 12.9%; $P = 0.001$), without having any significant effect on their decay time, in six cells tested (Fig. 8I). In line with findings obtained in parasagittal slices, bath application of SKF 89976A or SNAP 5114 alone or in combination did not alter the amplitude, frequency or half-decay time of mIPSCs in GP neurons (data not shown).

These results suggest that, under the present experimental conditions, GAT-1 and GAT-3 regulate GABA-mediated effects at striato-pallidal synapses preferentially over those generated by intrinsic GABAergic connections between GP neurons.

GAT-1 and GAT-3 blockade induces tonic currents in GP neurons

The results described so far demonstrate that GAT-1 and GAT-3 regulate synaptic $GABA_A$ receptor-mediated phasic inhibition in the rat GP. To examine whether GAT-1 and GAT-3 also modulate extrasynaptic $GABA_A$-mediated tonic inhibition in the rat GP, we conducted two series of experiments. In light of previous studies showing that bath application of $GABA_A$ receptor antagonists (picrotoxin or bicuculline) abolishes sIPSCs and reduces holding currents in cerebellar, cortical and hippocampal neurons (Brickley *et al.*, 1996; Salin & Prince, 1996; Semyanov *et al.*, 2003; Scimemi *et al.*, 2005), we measured the baseline holding currents in GP neurons under control conditions or in the presence of bicuculline (20 μM). These experiments revealed that bicuculline-induced $GABA_A$ receptor blockade completely abolished sIPSCs, but did not have any significant effect on the baseline holding currents (107 ± 6.9%; $P = 0.69$; $n = 7$), of rat GP neurons (Fig. 9D and Supporting Information Fig. S2). Next, we examined whether blockade of GAT-1 or GAT-3 or the combined blockade of both transporters produced bicuculline-sensitive tonic inihibition of GP neurons (Fig. 9A–E). In these experiments, GAT-1 (10 and 30 μM) or GAT-3 (10 and 30 μM) inhibitors were applied first for 7–10 min, and then together with bicuculline throughout the recordings. The application of bicuculline (10 μM) slightly increased holding currents in the presence of 10 μM SKF 89976A or 10 μM SNAP 5114, but the effects did not reach significance (Fig. 9D and E). However, application of bicuculline significantly enhanced holding currents in the presence of 30 μM SKF 89976A or 30 μM SNAP 5114, given alone or in combination (201 ± 34%, $n = 6$, $P = 0.01$; 199 ± 26%, $P = 0.001$, $n = 6$; and 610 ± 56%, $P = 0.001$, $n = 6$), respectively (Fig. 9C–E).

Taken together, our results suggest that GABA reuptake through GAT-1 and GAT-3 regulates extrasynaptic $GABA_A$ receptor-mediated tonic inhibition in the rat GP under normal physiological conditions.

Discussion

Our findings provide further evidence that GAT-1 and GAT-3 are differentially distributed and tightly regulate $GABA_A$-receptor mediated GABAergic synaptic transmission at striatopallidal synapses in the rat GP. From the electron microscopic and electrophysiological data presented in this study, four main conclusions can be drawn about the localization and function of GATs in the GP: (i) GAT-1 and GAT-3 are differentially distributed, thereby providing largely complementary target sites for GABA reuptake, in the rat GP – GAT1 mediates its effects mainly through neuronal reuptake at the pre-terminal level, whereas GAT-3 acts predominantly through glial processes; (ii) GAT-1 selectively modulates the decay time of striatal eIPSCs, whereas GAT-3 regulates both the amplitude and decay time of eIPSCs, in rat GP neurons following striatal stimulation; (iii) both GAT-1 and GAT-3 modulate the amplitude and frequency of sIPSCs, but have no significant effect on mIPSCs, in the rat GP; and (iv) both GAT-1 and GAT-3 regulate $GABA_A$ receptor-mediated tonic currents in the GP. Together, these findings demonstrate the differential patterns of distribution and the complementary functions of GAT-1 and GAT-3 in the regulation of GABAergic transmission in the rat GP. Knowing the importance of increased GABAergic outflow to the GP in the pathophysiology of Parkinson's disease, GATs may be considered as potential targets for the future development of antiparkinsonian agents that could increase GAT-1-mediated or GAT-3-mediated GABA reuptake functions in pathological conditions.

GAT-1 and GAT-3 activity shapes GABAergic synaptic transmission in GP neurons

Several studies have demonstrated that bath application of GAT-1 inhibitors (NO711 or tiagabine) dramatically prolongs the decay, but not the amplitude, of large eIPSCs in hippocampal neurons (Roepstorff & Lambert, 1992, 1994; Thompson & Gähwiler, 1992; Isaacson *et al.*, 1993; Draguhn & Heinemann, 1996; Overstreet & Westbrook, 2003) and cerebral cortex (Gonzalez-Burgos *et al.*, 2009). In the present study, we used SKF 89976A, which was previously shown to reduce the activity of monkey pallidal neurons *in vivo* (Galvan *et al.*, 2005), as a GAT-1 inhibitor. In line with the results reported from hippocampal slices, our data demonstrate that bath application of 10 μ_M SKF 89976A increases the decay, but not the amplitude, of large eIPSCs in the rat GP, thereby supporting the notion that the neuronal GAT regulates GABA clearance during strong activation of GABAergic afferents (Isaacson *et al.*, 1993; Roepstorff & Lambert, 1994; Overstreet & Westbrook, 2003). In the rat GP, as in the monkey external GP (Galvan *et al.*, 2005), the predominant sites of GAT-1-mediated GABA reuptake are most likely pre-terminal segments of striatopallidal axons. Although the exact source of the GAT-1-immunoreactive unmyelinated axons was not demonstrated in the present study, their abundance and widespread distribution throughout the GP suggest that they mainly originate from the STR.

Most studies of GAT functions have focused on the role of GAT-1 in the regulation of GABA levels in various CNS regions. However, as shown in the present study, GAT-3 is also expressed in several areas of the mammalian brain, primarily in glia, where it may play important roles in the clearance of extracellular GABA (see also Durkin *et al.*, 1995; Minelli *et al.*, 1996). Recent studies have, indeed, demonstrated that GAT-3 modulates GABAergic

synaptic transmission in the rat neocortex (Keros & Hablitz, 2005; Kinney, 2005) and STR (Kirmse *et al.*, 2009). In line with these observations, our results show that SNAP 5114 (10 μ_M) increases the amplitude and prolongs the decay time of eIPSCs in the rat GP. Although 10 μ_M SNAP 5114 may also block GAT-2 (Borden, 1996), the fact that there is no evidence for significant GAT-2 expression in the rodent pallidum (Ikegaki *et al.*, 1994; Durkin *et al.*, 1995; Yasumi *et al.*, 1997) strongly suggests that the effects of SNAP 5114 in the rat GP are mainly mediated through blockade of GAT-3 GABA reuptake mechanisms.

The mechanisms by which GAT-3 blockade increases the amplitude of eIPSCs in the GP remain empirical. However, in light of studies showing that GABA can depolarize GABAergic medium spiny neurons (Mercuri *et al.*, 1991; Blackwell *et al.*, 2003; Bracci & Panzeri, 2006; Ade *et al.*, 2008), and that blockade of tonic conduction in striatopallidal neurons decreases their excitability (Ade *et al.*, 2008), it is possible that the increase in amplitude of eIPSCs in response to GAT-3 blockade simply results from the activation of a larger number of GABAergic medium spiny neurons and interneurons by striatal stimulation in the presence of a GAT-3 blocker. In addition, as the amplitude of eIPSCs could be increased through various mechanisms, including multi-vesicular transmitter release, slower deactivation of postsynaptic $GABA_A$ receptors or decreased sensitization of $GABA_A$ receptors, future studies are needed to determine whether GAT-3 has any significant influences on these mechanisms. Because GAT-1 and GAT-3 are the only two GATs in the rodent pallidum (Ikegaki *et al.*, 1994; Durkin *et al.*, 1995; Yasumi *et al.*, 1997), blockade of both transporters was found to have stronger effects on eIPSCs than GAT-1 or GAT-3 blockade alone, suggesting that the two transporters play complementary functions in the regulation of extrasynaptic GABA diffusion in the rat GP.

GAT-1 and GAT-3 modulate sIPSCs in the rat GP

In light of our data, it appears that the effects of GAT-1 blockade on sIPSCs vary across brain regions. For instance, application of NO711, or the use of GAT-1-deficient mice, has revealed no significant effect of GAT-1 blockade on sIPSCs in the neocortex and hippocampus (Jensen *et al.*, 2003; Keros & Hablitz, 2005; Bragina *et al.*, 2008), whereas other data from the cerebellum, together with our current findings in the rat GP, suggest the opposite (Chen & Yung, 2003; Chiu *et al.*, 2005). It is unlikely that these variable effects are caused by differences in GAT blocker specificity, because the GAT-1 inhibitors used in these studies, NO711 and SKF 89976A, are both highly potent and selective for GAT-1 (Borden, 1996). It is also unlikely that the lack of effect in GAT-1-deficient mice was attributable to compensatory changes in response to the chronically elevated extracellular GABA concentration, because the levels of GAD65, vesicular GAT, the $GABA_A$ receptor $\alpha 1$ subunit, $GABA_B$ receptors, GAT-2 and GAT-3 in these animals were not different from those found in normal mice (Jensen *et al.*, 2003; Chiu *et al.*, 2005; Bragina *et al.*, 2008).

As discussed above, GABA can have depolarizing effects on striatal projection neurons (Bracci & Panzeri, 2006; Ade *et al.*, 2008) that can be accentuated and generated in large populations of medium spiny neurons by the excess of extracellular GABA induced by blockade of GAT-1 and GAT-3. As striatopallidal axons give rise to profuse terminal arborization in the GP (Kawaguchi *et al.*, 1990), this widespread striatal activation could

underlie the increased frequency and amplitude of sIPSCs, but not mIPSCs, in the GP. Another mechanism that could possibly mediate these effects is a reduction of non-vesicular release of GABA through GAT-1, as demonstrated in the hippocampus (Richerson & Wu, 2003; Wu *et al.*, 2007). Such an effect on GABA release from striatal interneurons or glia in the STR could lead to reduced tonic inhibition of medium spiny neurons, and thereby increased amplitude of sIPSCs in the GP.

In line with previous results from the neocortex (Kinney, 2005), SNAP 5114 application increased the amplitude and frequency of sIPSCs in the rat GP, suggesting that both neuronal and glial GAT-1 as well as glial GAT-3 play a significant modulatory role in GABAergic transmission in the GP and neocortex (see also Ng *et al.*, 2000; Galvan *et al.*, 2005). The respective roles of the different transporters under normal and pathological conditions remain to be established. Although the exact mechanisms by which both GATs modulate sIPSCs in the rat GP and the cerebellum, but not in the hippocampus, remain unclear, various factors, including the expression level and pharmacological properties of postsynaptic $GABA_A$ receptors and the level of activity and relative abundance of presynaptic release sites of GABA, are potential variables that could contribute to these differential effects across brain regions. Thus, because the functional effects of GAT-1 on sIPSCs are specific to brain regions, the translation of data obtained in a particular population of neurons to another must be performed with great caution.

GAT-1 and GAT-3 modulation of GABAergic transmission in the rat GP is action potential-dependent

Our findings demonstrate that the GAT-1 inhibitor does not significantly affect mIPSCs in the rat GP, a result different from that of a previous study showing that tigabine, a GAT-1 selective blocker, prolonged the decay and reduced the frequency of mIPSCs in rat GP neurons (Chen & Yung, 2003). On the other hand, it is noteworthy that our findings are in line with previous studies in slices of rat hippocampus (Thompson & Gähwiler, 1992; Overstreet & Westbrook, 2003) and data gathered from different brain regions in GAT-1-deficient mice (Jensen *et al.*, 2003), showing a lack of effect of GAT-1 on mIPSCs. It is unlikely that this apparent discrepancy is the result of differential effects of the two antagonists used in these studies on GAT-1, because the relative affinities and specificities of tigabine and SKF 89976A for GAT-1 are similar (Borden, 1996). One possibility is that different populations of GP neurons have been recorded in these two studies. Rat GP neurons can, indeed, be separated into two functional domains: the ‘inner’ neurons, located medially, receive twice as many inputs from other GP neurons than the ‘outer’ neurons, located along the border between the STR and GP (Sadek *et al.*, 2007). Because most of our recordings were performed in outer GP neurons, it is possible that different locations of GP recording sites between our study and that of Chen & Yung (2003) explain the discrepancy between these two sets of data. Another explanation could be that recordings were made from two physiologically different populations of GP neurons in these studies. However, although pallidal neurons can, indeed, be segregated into two major subtypes on the basis of their physiological properties (Nambu & Llinas, 1994; Cooper & Stanford, 2000), previous data from our laboratory and others, using similar slice preparations, revealed that the overwhelming majority of GP neurons in brain slices display the electrophysiological

properties of the so-called type II cells (Poisik *et al.*, 2003; Jin *et al.*, 2006). Thus, although we did not attempt to characterize the specific neuronal phenotype that we recorded from in the present study, it appears reasonable to suggest that the vast majority of neurons recorded in both studies are of the type II family subtype, thereby ruling out the possibility that the effects of GAT blockade on mIPSCs could be merely explained by recordings being made in different neuronal populations. We also could not show any significant effect of SNAP 5114 on mIPSCs, similar to previous reports based on recordings in cortical slices (Kinney, 2005). Thus, our results support the idea that GAT-1 and GAT-3 are selectively involved in the modulation of action potential-dependent GABAergic transmission at striatopallidal synapses.

GAT-1 and GAT-3 regulate preferentially striatopallidal GABAergic transmission

Because electrical stimulation in the STR could activate both GABAergic striatopallidal axons and recurrent axon collaterals of pallidostriatal projections (Kita & Kitai, 1991; Bevan *et al.*, 1998; Smith *et al.*, 1998; Kita *et al.*, 1999; Kita & Kita, 2001; Sadek *et al.*, 2007), the effects of GAT-1 or GAT-3 blockade on eIPSCs and sIPSCs recorded in the GP after striatal stimulation could result from modulation of extrinsic striatopallidal transmission and/or regulation of local intrapallidal collaterals of pallidostriatal axons. Although this possibility can be tested by the dual recording of functionally connected pairs of GP neurons, the probability of finding such pairs in the normal GP is low (Oorschot, 1996; Bar-Gad *et al.*, 2003; Sadek *et al.*, 2007). To partly overcome such a problem, we recorded IPSCs evoked in GP neurons by local intrapallidal stimulation in coronal slices of the striatopallidal complex, assuming that, in such a preparation, striatopallidal axons have been severely damaged and that eIPSCs in the GP are largely mediated by GABA release from intrinsic axon collaterals of GP neurons (Cooper & Stanford, 2001; Valenti *et al.*, 2003). In contrast to results gathered from striatal stimulation-mediated events in parasagittal slices, bath application of GAT inhibitors did not affect the amplitude or decay of eIPSCs in GP neurons after local stimulation in coronal slices. Blockade of either GAT-1 or GAT-3 also had no significant effect on sIPSCs under these conditions, but the decay and amplitude of sIPSCs were significantly increased when both GAT-1 and GAT-3 were blocked. Together, these results suggest that, under the *in vitro* experimental conditions used in our study, GAT-1 and GAT-3 exert a more powerful effect on the modulation of extrinsic GABAergic striatopallidal transmission than on the local intrinsic GABAergic microcircuitry of axon collaterals of pallidostriatal neurons. However, our findings do not rule out the possibility that GAT function may be dynamically regulated, and play key roles in regulating intrinsic pallido-pallidal GABAergic connections in specific behavioral states. Future *in vivo* studies are warranted to examine this issue further in awake whole animals with intact basal ganglia circuitry.

GAT-1 and GAT-3 regulation of tonic $GABA_A$ receptor-mediated inhibition in the GP

Tonic $GABA_A$ receptor-mediated currents have been described in cerebellar granule cells, dentate gyrus granule cells and hippocampal interneurons (Semyanov *et al.*, 2004). Application of $GABA_A$ receptor antagonists was found to reduce the holding currents and abolish sIPSCs in these neurons. Our data revealed no clear evidence for tonic activation of postsynaptic $GABA_A$ receptor-mediated currents in rat GP neurons, suggesting that the

ambient GABA concentration may be low in our preparation. On the other hand, the tonic inhibition of specific neuronal populations is developmentally regulated (Brickley *et al.*, 1996; Wall & Usowicz, 1997; Demarque *et al.*, 2002). For instance, the tonic inhibition of cerebellar granule cells is weak early in postnatal development (P6–14), but much stronger at later stages (P19–21) (Brickley *et al.*, 1996; Wall & Usowicz, 1997; Demarque *et al.*, 2002). A recent study demonstrated that tonic inhibition is detected at P12–14 up to P19–34 in projection neurons of the mouse STR (Kirmse *et al.*, 2008). Although unlikely, it is possible that the expression of tonic $GABA_A$ receptor-mediated inhibition in the rat GP was still too low to be detected in brain slices of the P14–17 rats used in our study. Further experiments in older rats would be needed to address this issue.

The tonic $GABA_A$ receptor-mediated inhibition is modulated by GAT-1 in the neostriatum and hippocampus (Semyanov *et al.*, 2003; Scimemi *et al.*, 2005; Kirmse *et al.*, 2008). Bicuculline-dependent tonic currents can, in fact, be induced or increased in hippocampal pyramidal cells (Jensen *et al.*, 2003) and cerebellar Purkinje cells (Chiu *et al.*, 2005) of GAT-1-deficient mice or after blockade of GAT-1 in the neostriatum (Kirmse *et al.*, 2008). In line with these studies, we demonstrated the expression of tonic $GABA_A$ receptor-mediated inhibition of GP neurons after blockade of GAT-1 or GAT-3 with high concentrations of their respective antagonists. Tonic currents of higher amplitude were induced when both GAT-1 and GAT-3 were blocked, thereby suggesting that the two transporters contribute to this physiological effect in the rat GP. Similar findings were reported in the rat neocortex after dual blockade of GAT-1 and GAT-3 (Keros & Hablitz, 2005). On the basis of our ultrastructural data showing that GAT-1 and GAT-3 are strongly expressed throughout the rat and monkey GP (Galvan *et al.*, 2005), it is not surprising that blockade of both transporters has the strongest effects on $GABA_A$ receptor-mediated currents in rat GP neurons.

Functional and therapeutic relevance of GATs in the GP

The present study provides strong evidence that GAT-1 and GAT-3 modulate $GABA_A$ receptor-mediated synaptic (phasic) and extrasynaptic (tonic) inhibition in the GP. Overactivity of GABAergic transmission in the GP is one of the cardinal pathophysiological features of Parkinson's disease (DeLong, 1990). In light of a recent study showing that adenosine inhibits GAT-1-mediated GABA uptake in the rat GP (Gonzalez *et al.*, 2006), combined with the fact that A2A receptor antagonists have significant antiparkinsonian effects (Kanda *et al.*, 2000; Chase *et al.*, 2003), it is possible that the antiparkinsonian effects of A2A receptor antagonists are partly attributable to the presynaptic modulation of GABA release at striatopallidal synapses through facilitation of GAT-1 function. GABA uptake is also modulated through activation of CB1 receptors in the rat GP (Venderova *et al.*, 2005), providing another mechanism (Romero *et al.*, 2002; Brotchie, 2003) that could be used to regulate the overactive GABAergic striatopallidal transmission in Parkinson's disease. Thus, the direct and indirect modulation of GATs represents a highly promising therapeutic strategy that could be considered in the treatment of brain diseases characterized by abnormal upregulation of GABAergic neurotransmission.

Supplementary Material

Refer to Web version on PubMed Central for supplementary material.

Acknowledgements

This research was supported by NIH grants R01 NS 0432937 and the Yerkes National Primate Center NIH/NCRR base grant (RR-00165). We thank Susan Jenkins for technical assistance. Drs Adriana Galvan and Thomas Wichmann are also thanked for their critical reading of the manuscript.

Abbreviations

ACSF	artificial cerebrospinal fluid
CNQX	6-cyano-7-nitroquinoxaline-2,3-dione
CNS	central nervous system
D-AP5	D-(−)-2-amino-5-phosphonopen-tanoic acid
eIPSC	evoked inhibitory postsynaptic current
GAT	GABA transporter
GAT-1	GABA transporter subtype 1
GAT-2	GABA transporter subtype 2
GAT-3	GABA transporter subtype 3
GP	globus pallidus
IPSC	inhibitory postsynaptic current
mIPSC	miniature inhibitory postsynaptic current
P	postnatal day
PB	phosphate buffer
PBS	phosphate-buffered saline
QX314	*N*-(2,6-dimethylphenylcarbamoylmethyl)-triethylammonium bromide
SEM	standard error of the mean
sIPSC	spontaneous inhibitory postsynaptic current
SKF 89976A	1-(4,4-diphenyl-3-butenyl)-3-piperidine-carboxylic acid hydrochloride
SNAP 5114	1-(2-[tris(4-methoxyphenyl)meth-oxy]ethyl)-(*S*)-3-piperidinecarboxylic acid
STR	striatum
TTX	tetrodotoxin

References

Ade KK, Janssen MJ, Ortinski PI, Vivini S. Differential tonic GABA conductances in striatal medium spiny neurons. J. Neurosci. 2008; 28:1185–1197. [PubMed: 18234896]

Allen NJ, Rossi DJ, Attwell D. Sequential release of GABA by exocytosis and reversed uptake leads to neuronal swelling in simulated ischaemia of hippocampal slices. J. Neurosci. 2004; 24:3837–3849.

Andrade R. Blockade of neurotransmitter-activated K^+ conductance by QX-314in the rat hippocampus. Eur. J. Pharmacol. 1991; 199:259–262. [PubMed: 1659537]

Bar-Gad I, Heimer G, Ritov Y, Bergman H. Functional correlations between neighboring neurons in the primate globus pallidus are weak or nonexistent. J. Neurosci. 2003; 23:4012–4016. [PubMed: 12764086]

Bevan MD, Booth PA, Eaton SA, Bolam JP. Selective innervation of neostriatal interneurons by a subclass of neuron in the globus pallidus of the rat. J. Neurosci. 1998; 18:9438–9452. [PubMed: 9801382]

Bevan MD, Magill PJ, Terman D, Bolam JP, Wilson CJ. Move to the rhythm: oscillations in the subthalamic nucleus-external globus pallidus network. Trends Neurosci. 2002; 25:525–531. [PubMed: 12220881]

Blackwell KT, Czubayko U, Plenz D. Quantitative estimate of synaptic inputs to striatal neurons during up and down state *in vitro*. J. Neurosci. 2003; 23:9123–9132. [PubMed: 14534246]

Borden LA. GABA transporter heterogeneity: pharmacology and cellular localization. Neurochem. Int. 1996; 29:335–356. [PubMed: 8939442]

Bracci E, Panzeri S. Excitatory GABAergic effects in striatal projection neurons. J. Neurophysiol. 2006; 95:1285–1290. [PubMed: 16251264]

Bragina L, Marchionni I, Omrani A, Cozzi A, Pellegrini-Giampietro DE, Cherubini E, Conti F. GAT-1regulates both tonic and phasic GABAA receptor-mediated inhibition in the cerebral cortex. J. Neurochem. 2008; 105:1781–1793. [PubMed: 18248614]

Brickley SG, Cull-Candy SG, Farrant M. Development of a tonic form of synaptic inhibition in rat cerebellar granule cells resulting from persistent activation of $GABA_A$ receptors. J. Physiol. 1996; 497:753–759. [PubMed: 9003560]

Brotchie JM. CB1 cannabinoid receptor signalling in Parkinson's disease. Curr. Opin. Pharmacol. 2003; 3:54–61. [PubMed: 12550742]

Calcagnotto ME, Paredes MF, Baraban SC. Heterotopic neurons with altered inhibitory synaptic function in an animal model of malformation-associated epilepsy. J. Neurosci. 2002; 22:7596–7605. [PubMed: 12196583]

Chase TN, Bibbiani F, Bara-Jimenez W, Dimitrova T, Oh-Lee JD. Translating A_{2A} antagonist KW6002 from animal models to parkinsonian patients. Neurology. 2003; 61:S107–S111. [PubMed: 14663022]

Chen L, Yung WH. Effects of the GABA-uptake inhibitor tiagabine in rat globus pallidus. Exp. Brain Res. 2003; 152:263–269. [PubMed: 12879169]

Chiu CS, Brickley S, Jensen K, Sputhwell A, Mckinney S, Candy SC, Mody I, Laster HA. GABA transporter deficiency causes tremor, ataxia, nervousness, and increased GABA induced tonic conductance in cerebellum. J. Neurosci. 2005; 25:3234–3245. [PubMed: 15788781]

Conti F, Melone M. De. Biasi S, Minelli A, Brecha NC, Ducati A. Neuronal and glial localization of GAT-1,a high-affinity gamma-aminobutyric acid plasma membrane transporter, in human cerebral cortex: with a note on its distribution in monkey cortex. J. Comp. Neurol. 1998; 396:51–63. [PubMed: 9623887]

Cooper AJ, Stanford IM. Electrophysiological and morphological characteristics of three subtypes of rat globus pallidus neurones *in vitro*. J. Physiol. 2000; 527:291–304. [PubMed: 10970430]

Cooper AJ, Stanford IM. Dopamine D2 receptor mediated presynaptic inhibition of striatopallidal GABA(A) IPSCs *in vitro*. Neuro-physiology. 2001; 41:62–72.

DeLong MR. Primate models of movement disorders of basal ganglia origin. Trends Neurosci. 1990; 13:281–285. [PubMed: 1695404]

Demarque M, Represa A, Becq H, Khalilov I, Ben-Ari Y, Aniksztejin L. Paracrine intercellular communication by a Ca^{2+}- and SNARE-independent release of GABA and glutamate prior to synapse formation. Neuron. 2002; 36:1051–1061. [PubMed: 12495621]

Draguhn A, Heinemann U. Different mechanisms regulate IPSC kinetics in early postnatal and juvenile hippocampal granule cells. J. Neurophysiol. 1996; 76:3983–3993. [PubMed: 8985894]

Durkin MM, Smith KE, Borden LA, Weinshank RL, Branchek TA, Gustafson EL. Localization of messenger RNAs encoding three GABA transporters in rat brain: an *in situ* hybridization study. Brain Res. Mol. Brain Res. 1995; 33:7–21. [PubMed: 8774941]

Engel D, Schmitz D, Gloveli T, Frahm C, Heinemann U, Draguhn A. Laminar difference in GABA uptake and GAT-1expression in rat CA1. J. Physiol. 1998; 512:643–649. [PubMed: 9769410]

Galvan A, Villalba RM, West SM, Maidment NT, Ackerson LC, Smith Y, Wichmann T. GABAergic modulation of the activity of globus pallidus neurons in primates: *in vivo* analysis of the functions of GABA receptors and GABA transporters. J. Neurophysiol. 2005; 94:990–1000. [PubMed: 15829599]

Gonzalez B, Paz F, Floran L, Aceves J, Erlij D, Floran B. Adenosine A_{2A} receptor stimulation decreases GAT-1-mediated GABA uptake in the globus pallidus of the rat. Neuropharmacology. 2006; 51:154–159. [PubMed: 16730753]

Gonzalez-Burgos G, Rotaru DC, Zaitsev AV, Povysheva NV, Lewis DA. GABA transporter GAT1 prevents spillover at proximal and distal GABA synapses onto primate prefrontal cortex neuron. J. Neurophysiol. 2009; 101:533–547. [PubMed: 19073797]

Ikegaki N, Saito N, Hashima M, Tanaka C. Production of specific antibodies against GABA transporter subtypes (GAT1, GAT2, GAT3) and their application to immunocytochemistry. Mol. Brain Res. 1994; 26:47–54. [PubMed: 7854065]

Isaacson JS, Solis JM, Nicoll RA. Local and diffuse synaptic actions of GABA in the hippocampus. Neuron. 1993; 10:165–175. [PubMed: 7679913]

Jensen K, Chiu CS, Sokolova I, Lester HA, Mody I. GABA transporter-1 (GAT-1)-deficient mice: differential tonic activation of GABAA versus GABAB receptors in the hippocampus. J. Neurophysiol. 2003; 90:2690–2701. [PubMed: 12815026]

Jin XT, Smith Y. Activation of presynaptic kainate receptors suppresses GABAergic synaptic transmission in the rat globus pallidus. Neuroscience. 2007; 149:338–349. [PubMed: 17881134]

Jin XT, Pare JF, Raju DV, Smith Y. Localization and function of pre- and postsynaptic kainate receptors in the rat globus pallidus. Eur. J. Neurosci. 2006; 23:374–386. [PubMed: 16420445]

Kanda T, Jackson MJ, Smith LA, Pearce RK, Nakamura J, Kase H, Kuwana Y, Jenner P. Combined use of the adenosine A(2A) antagonist KW-6002with L-DOPA or with selective D1 or D2 dopamine agonist increases antiparkinsonian activity but not dyskinesia in MPTP-treated monkeys. Exp. Neurol. 2000; 162:321–327. [PubMed: 10739638]

Kawaguchi Y, Wilson CJ, Emson PC. Projection subtypes of rat neostriatal matrix cells revealed by intracellular injection of biocytin. J. Neurosci. 1990; 10:3421–3438. [PubMed: 1698947]

Keros S, Hablitz JJ. Subtype-specific GABA transporter antagonists synergistically modulate phasic and tonic GABAA conductances in rat neocortex. J. Neurophysiol. 2005; 94:2073–2085. [PubMed: 15987761]

Kinney GA. GAT-3transporters regulate inhibition in the neocortex. J. Neurophysiol. 2005; 94:4533–4537. [PubMed: 16135550]

Kirmse K, Dvorzhak A, Kirischuk S, Grantyn R. GABA transporter 1 tunes GABAergic synaptic transmission at output neurons of the mouse neostriatum. J. Physiol. 2008; 586:5665–5678. [PubMed: 18832421]

Kirmse K, Kirischuk S, Grantyn R. Role of GABA transporter 3 in GABAergic synaptic transmission at striatal output neurons. Synapse. 2009; 63:921–929. [PubMed: 19588470]

Kita H, Kita T. Number, origins, and chemical types of rat pallidostriatal projection neurons. J. Comp. Neurol. 2001; 437:438–448. [PubMed: 11503145]

Kita H, Kitai ST. Intracellular study of rat globus pallidus neurons: membrane properties and responses to neostriatal, subthalamic and nigral stimulation. Brain Res. 1991; 564:296–305. [PubMed: 1810628]

Kita H, Tokuno H, Nambu A. Monkey globus pallidus external segment neurons projecting to the neostriatum. NeuroReport. 1999; 10:1467–1472. [PubMed: 10380964]

McLean HA, Caillard O, Khazipov R, Ben-Ari Y, Gaiarsa JL. Spontaneous release of GABA activates $GABA_B$ receptors and controls network activity in the neonatal rat hippocampus. J. Neurophysiol. 1996; 76:1036–1046. [PubMed: 8871218]

Mercuri NB, Calabresi P, Stefani A, Stratta F, Bernardi G. GABA depolarizes neurons in the rat striatum: an *in vivo* study. Synapse. 1991; 8:38–40. [PubMed: 1871679]

Minelli A, Brecha NC, Karschin C, DeBiasi S, Conti F. GAT-1,a high-affinity GABA plasma membrane transporter, is localized to neurons and astroglia in the cerebral cortex. J. Neurosci. 1995; 15:7734–7746. [PubMed: 7472524]

Minelli A, DeBiasi S, Brecha NC, Zuccarello LV, Conti F. GAT-3,a high-affinity GABA plasma membrane transporter, is localized toastrocytic processes, and it is not confined to the vicinity of GABAergic synapses in the cerebral cortex. J. Neurosci. 1996; 16:6255–6264. [PubMed: 8815906]

Nambu A, Llinas R. Electrophysiology of globus pallidus neurons *in vitro*. J. Neurophysiol. 1994; 72:1127–1139. [PubMed: 7807199]

Nathan T, Jensen MS, Lambert JD. The slow inhibitory postsynaptic potential in rat hippocampal CA1 neurons is blocked by intracellular injection of QX-314. Neurosci. Lett. 1990; 110:309–313. [PubMed: 2325903]

Ng CH, Wang XS, Ong WY. A light and electron microscopic study of the GABA transporter GAT-3in the monkey basal ganglia and brainstem. J. Neurocytol. 2000; 29:595–603. [PubMed: 11283414]

Nusser Z, Mody I. Selective modulation of tonic and phasic inhibitions in dentate gyrus granule cells. J. Neurophysiol. 2002; 87:2624–2628. [PubMed: 11976398]

Oorschot DF. Total number of neurons in the neostriatal, pallidal, subthalamic, and substantia nigral nuclei of the rat basal ganglia: a stereological study using the cavalieri and optical disector methods. J. Comp. Neurol. 1996; 366:580–599. [PubMed: 8833111]

Overstreet LS, Westbrook GL. Synaptic sensity regulates independence at unitary inhibitory synapses. J. Neurosci. 2003; 23:2618–2626. [PubMed: 12684447]

Overstreet LS, Jones MV, Westbrook GL. Slow desensitization regulates the availability of synaptic GABA(A) receptors. J. Neurosci. 2000; 20:7914–7921. [PubMed: 11050111]

Parent A, Charara A, Pinault D. Single striatofugal axons arborizing in both pallidal segments and in the substantia nigra in primates. Brain Res. 1995; 698:280–284. [PubMed: 8581498]

Peters, A.; Palay, S.; Webster, HD. The Fine Structure of the Nervous System. Oxford University Press; New York: 1991.

Plenz D, Kitai ST. A basal ganglia pacemaker formed by the subthalamic nucleus and external globus pallidus. Nature. 1999; 400:677–682. [PubMed: 10458164]

Poisik OV, Mammaioni G, Traynelis S, Smith Y, Conn PJ. Distinct functional roles of the metabotropic glutamate receptors 1 and 5 in the rat globus pallidus. J. Neurosci. 2003; 23:122–130. [PubMed: 12514208]

Raiteri L, Stigliani S, Zedda L, Raiteri M, Bonanno G. Multiple mechanisms of transmitter release evoked by ‘pathologically’ elevated ectracellular [K+]: involvement of transporter reversal and mitochondrial calcium. J. Neurochem. 2002; 80:706–714. [PubMed: 11841577]

Reynolds ES. The use of lead citrate at high pH as an electron-opaque stain in electron microscopy. J. Cell Biol. 1963; 17:208–212. [PubMed: 13986422]

Ribak CE, Tong WM, Brecha NC. GABA plasma membrane transporters, GAT-1 and GAT-3,display different distributions in the rat hippocampus. J. Comp. Neurol. 1996a; 367:595–606. [PubMed: 8731228]

Ribak CE, Tong WM, Brecha NC. Astrocytic processes compensate for the apparent lack of GABA transporters in the axon terminals of cerebellar Purkinje cells. Anat. Embryol. (Berl.). 1996b; 194:379–390. [PubMed: 8896702]

Richerson GB, Wu Y. Dynamic equilibrium of neurotransmitter transporters: not just for reuptake anymore. J. Neurophysiol. 2003; 90:1363–1374. [PubMed: 12966170]

Roepstorff A, Lambert JD. Comparison of the effect of the GABA uptake blockers, tiagabine and nipecotic acid, on inhibitory synaptic efficacy in hippocampal CA1 neurons. Neurosci. Lett. 1992; 146:131–134. [PubMed: 1337191]

Roepstorff A, Lambert JD. Factors contributing to the decay of the stimulus-evoked IPSC in rat hippocampal CA1 neurons. J. Neurophysiol. 1994; 72:2911–2926. [PubMed: 7897499]

Romero J, Lastres-Becker I, de Miguel R, Berrendero F, Ramos JA, Fernandez-Ruiz J. The endogenous cannabinoid system and the basal ganglia. Biochemical, pharmacological, and therapeutic aspects. Pharmacol. Ther. 2002; 95:137–152. [PubMed: 12182961]

Rossi DL, Hammann M, Attwell D. Multiple modes of GABAergic inhibition of rat cerebellar cells. J. Physiol. 2003; 548:97–110. [PubMed: 12588900]

Sadek AR, Magill PJ, Polam JP. A single-cell analysis of intrinsic connectivity in the rat globus pallidus. J. Neurosci. 2007; 27:6352–6362. [PubMed: 17567796]

Salin PA, Prince DA. Spontaneous $GABA_A$ receptor-mediated inhibitory currents in adult rat somatosensory cortex. J. Neurophysiol. 1996; 75:1573–1588. [PubMed: 8727397]

Scimemi A, Semyanov A, Sperk G, Kullmann DM, Walker MC. Multiple and plastic receptors mediate tonic $GABA_A$ receptor currents in the hippocampus. J. Neurosci. 2005; 25:10016–10024. [PubMed: 16251450]

Semyanov A, Walker MC, Kullmann DM. GABA uptake regulates cortical excitability via cell type-specific tonic inhibition. Nat. Neurosci. 2003; 6:484–490. [PubMed: 12679782]

Semyanov A, Walker MC, Kullmann DM, Silver RA. Tonically active $GABA_A$ receptor: modulating gain and maintaining the tone. Trends Neurosci. 2004; 27:262–269. [PubMed: 15111008]

Smith Y, Bevan MD, Shink E, Bolam JP. Microcircuitry of the direct and indirect pathways of the basal ganglia. Neuroscience. 1998; 86:353–387. [PubMed: 9881853]

Thompson SM, Gähwiler BH. Effects of the GABA uptake inhibitor tiagabine on inhibitory synaptic potentials in rat hippocampal slice cultures. J. Neurophysiol. 1992; 67:1698–1701. [PubMed: 1629773]

Valenti O, Marino MJ, Wittmann M, Lis E, DiLella AG, Kinney GG, Conn PJ. Group III metabotropic glutamatergic receptor-mediated modulation of the striatopallidal synapse. J. Neurosci. 2003; 23:7218–7226. [PubMed: 12904482]

Venderova K, Brown TM, Brotchie JM. Differental effects of endocannabinoids on [3H]-GABA uptake in the rat globus pallidus. Exp. Neurol. 2005; 194:284–287. [PubMed: 15899265]

Wall MJ, Usowicz MM. Development of action potential-dependent and independent spontaneous GABAA receptor-mediated currents in granule cells of postnatal rat cerebellum. Eur. J. Neurosci. 1997; 9:533–548. [PubMed: 9104595]

Wang XS, Ong WY. A light and electron microscopic study of GAT-1in the monkey basal ganglia. J. Neurocytol. 1999; 28:1053–1061. [PubMed: 11054905]

Wu Y, Wang W, Diez-Sampedro A, Richerson GB. Nonvesicular inhibitory neurotransmission via reversal of the GABA transporter GAT-1. Neuron. 2007; 56:851–865. [PubMed: 18054861]

Yasumi M, Sato K, Shimada S, Nishimura M, Tohyama M. Regional distribution of GABA transporter 1 (GAT1) mRNA in the rat brain: comparison with glutamic acid decarboxylase67 (GAD67) mRNA localization. Brain Res. Mol. Brain Res. 1997; 44:205–218. [PubMed: 9073162]

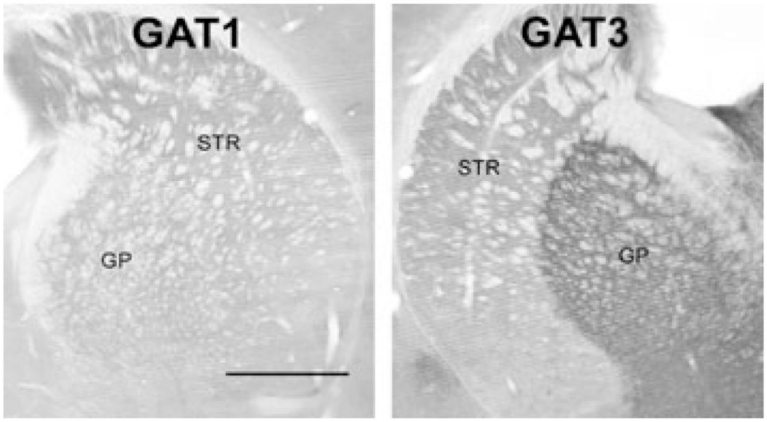

Fig. 1.

Light micrographs of GAT-1 and GAT-3 immunoreactivity in the striatopallidal complex of a P17 rat. Scale bar – 1.5 mm.

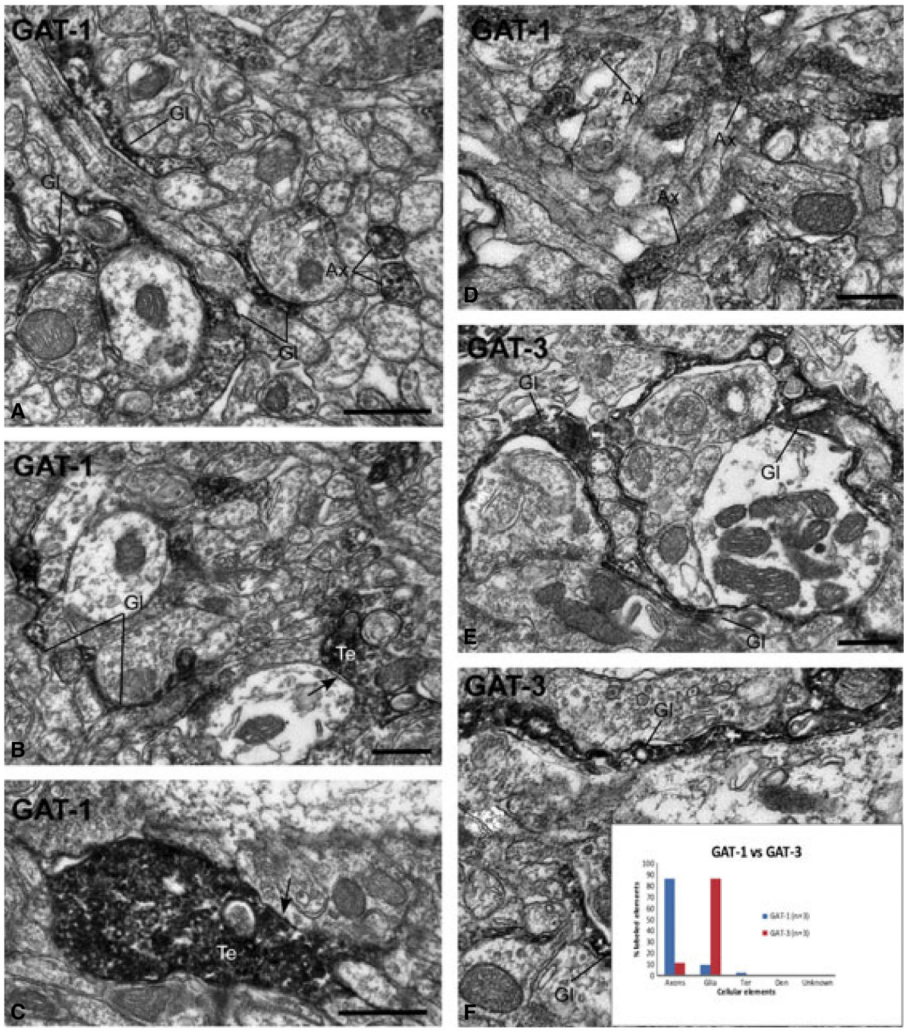

Fig. 2.

Electron micrographs of GAT-1-immunoreactive and GAT-3-immunoreactive elements in the GP of young (P15–20) rats. (A–D) GAT-1-positive unmyelinated axons (Ax), glial processes (Gl) and axon terminals (Te). (E–F) GAT-3-positive glial processes that ensheath unlabeled axon terminals. Scale bars – 0.5 μm. (G) Percentages of GAT-1-labeled and GAT-3-labeled neuronal and glial elements in the rat GP. Two young rats (P15–17) and one adult rat per group were used.

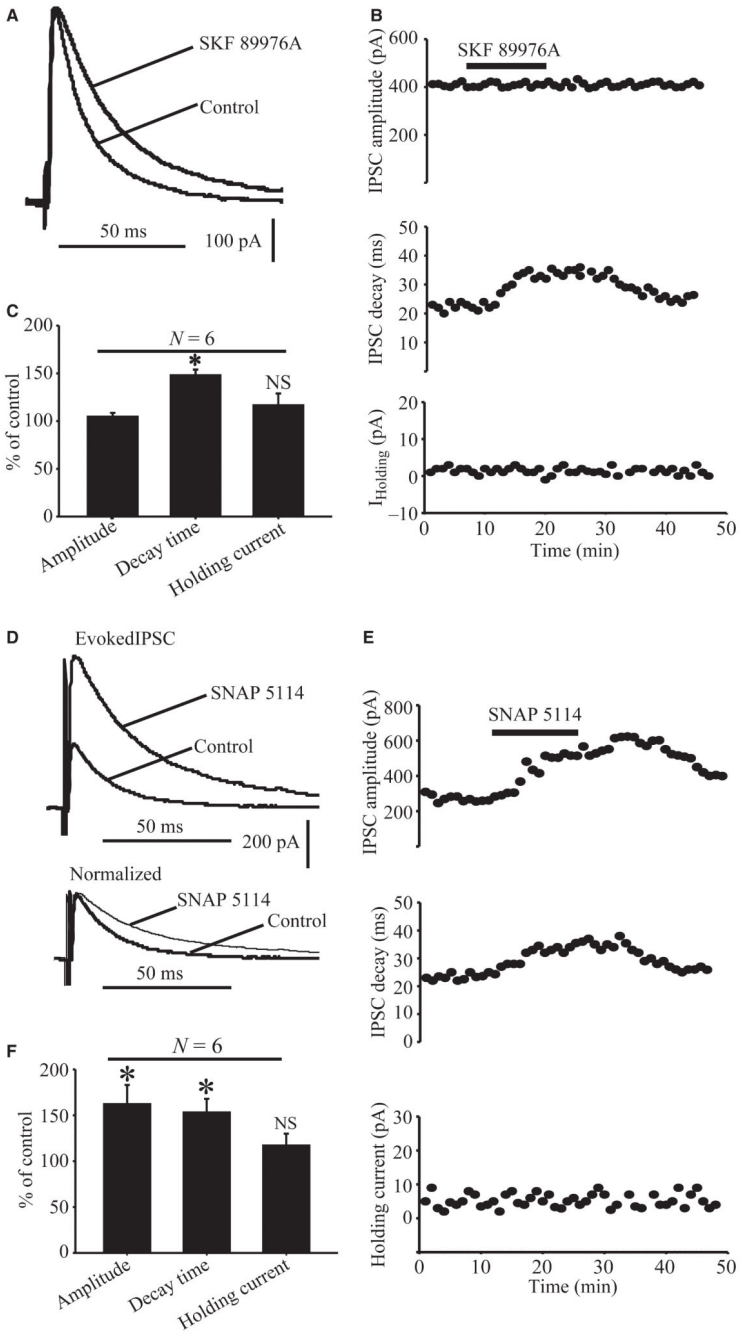

Fig. 3.

Effects of GAT-1 and GAT-3 blockade on evoked GABAergic synaptic transmission in the rat GP. (A) Application of SKF 89976A (10 μM) increases the decay time, but not the amplitude, of IPSCs evoked in GP neurons after striatal stimulation (15 V). (B) Effects of SKF 89976A application on time courses of amplitude (top), decay (middle) and baseline holding currents (bottom) of eIPSCs in the same neuron as in A. (C) Bar graph showing that SKF 89976A increases eIPSC decay time, but has no effect on the amplitude and baseline holding currents expressed as percentage of control ± SEM (*P = 0.002). (D) Upper traces

show that application of SNAP 5114 (10 μ_M) increases the amplitude and decay time of IPSCs evoked in GP neurons by 15-V striatal stimulation. The lower traces are the same as those above, except that the amplitude of the first IPSC recorded in the presence of SNAP 5114 has been normalized to the first IPSC recorded under control conditions. (E) The time course of eIPSC amplitude (top), decay time (middle) and holding currents (bottom) of the same neuron as in D in response to SNAP 5114 application. (F) Bar graph summarizing the effects of SNAP 5114 on eIPSC amplitude, decay time and holding current expressed as percentage of control ± SEM (*$P < 0.05$). *N*, number of cells tested; NS, not significant.

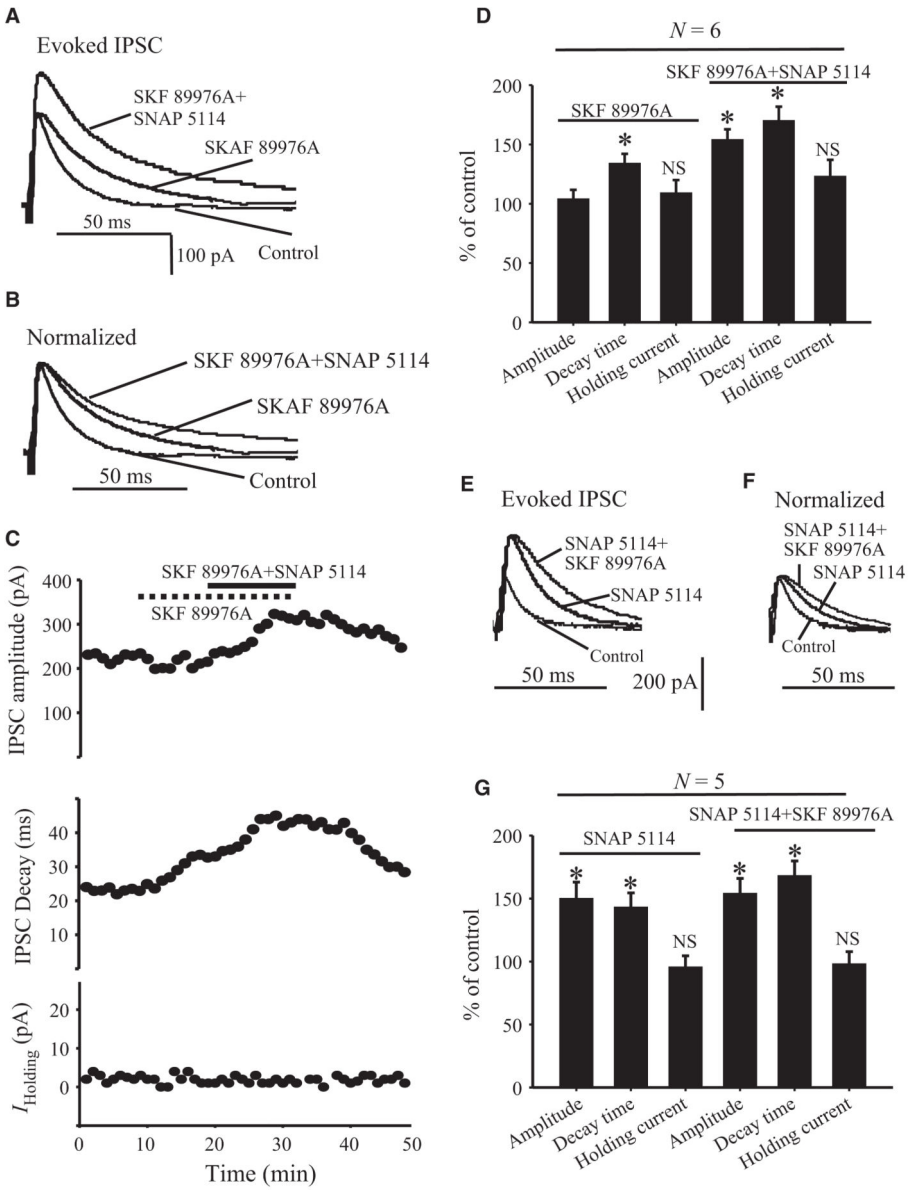

Fig. 4.

Effect of application of GAT-1 and GAT-3 inhibitors on evoked GABAergic synaptic transmission in the rat GP. (A) Application of SKF 89976A (10 μ_M) alone increases the decay time, but not the amplitude, of IPSCs evoked in GP neurons by striatal stimulation (15 V) (middle trace). Both the decay time and the amplitude of eIPSCs are increased in the presence of SKF 89976A and SNAP 5114 (top trace). (B) The IPSCs recorded in the presence of SKF 89976A and SKF 89976A plus SNAP 5114 have been normalized to the IPSCs recorded under control conditions. (C) Time course of eIPSC amplitude (top), decay time (middle) and holding currents (bottom) in response to application of SKF 89976A alone (dashed line) or SKF 89976A combined with SNAP 5114 (solid line). (D) Bar graph summarizing the effects of SKF 89976A alone or combined with SNAP 5114 on eIPSC amplitude, decay time and holding current expressed as percentage of control ± SEM (*P =

0.001) in response to striatal stimulation (15–20 V). (E) Application of SNAP 5114 alone (middle trace) increased both the amplitude and decay time (second trace) of eIPSCs. The decay time was further increased when SNAP 5114 was applied together with SKF 89976A (top trace). (F) The IPSCs recorded in the presence of SNAP 5114 and SNAP 5114 + SKF 89976A have been normalized to the IPSCs recorded under control conditions. (G) Bar graph summarizing the effects of SNAP 5114 alone or together with SKF 89976A on eIPSC amplitude, decay time and holding current expressed as percentage of control ± SEM (*P = 0.001). N, number of cells tested; NS, not significant.

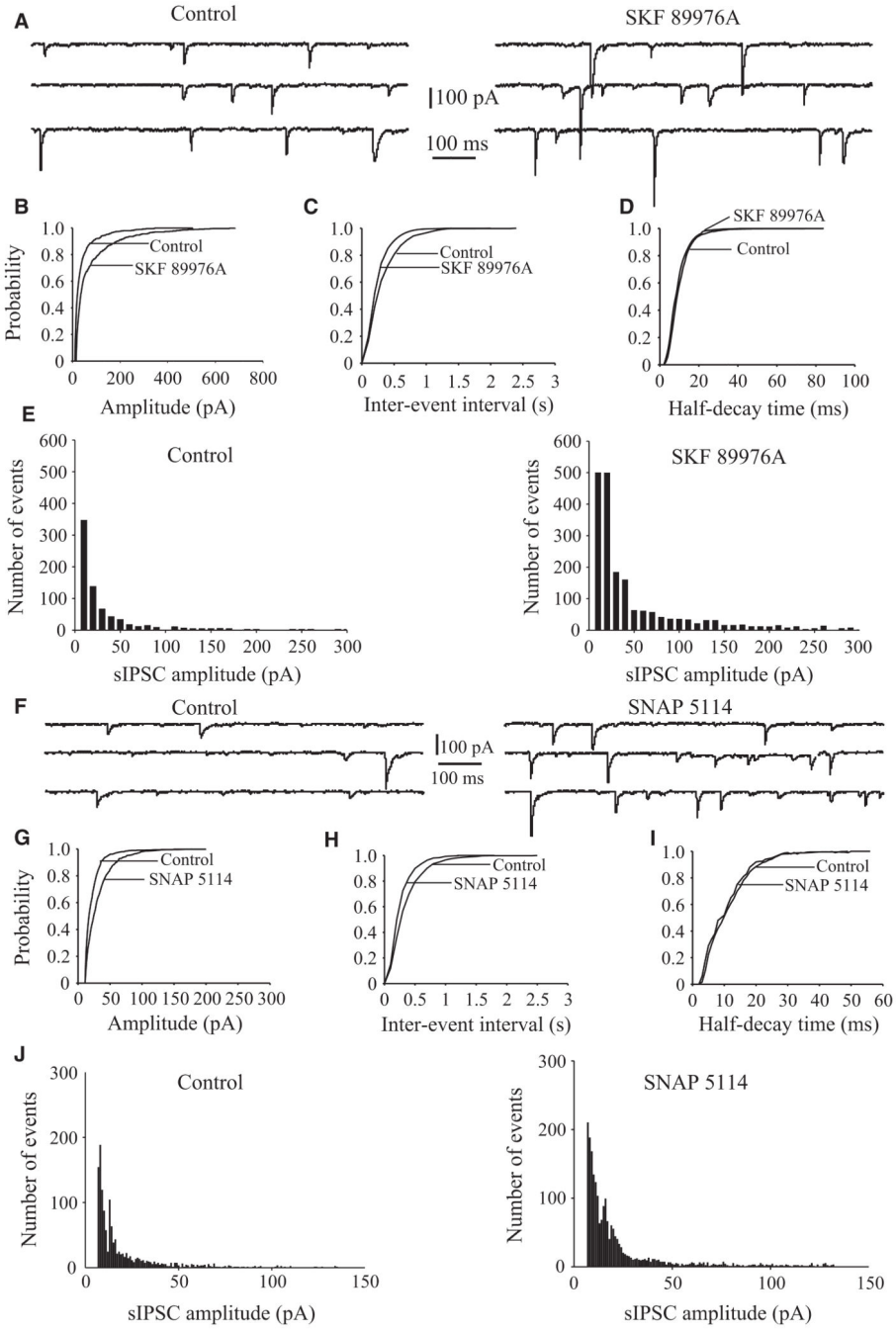

Fig. 5.

Effects of GAT-1 or GAT-3 blockers on sIPSCs in rat GP neurons. (A) Sample traces showing sIPSCs recorded in the presence of 50 μ_M CNQX and 50 μ_M D-AP5, under control conditions (left) and during bath application of SKF 89976A (10 μ_M) (right). (B–D) The cumulative distribution of the amplitude, inter-event interval and half-decay time of sIPSCs obtained from the same GP neuron as in A. SKF 89976A significantly shifts the amplitude distribution curve (B) to the right and the inter-event interval distribution curve (C) to the left ($P = 0.001$), but has no significant effect on the distribution of sIPSC half-decay time

(D, $P = 0.7$). (E) Amplitude distribution histograms of sIPSCs recorded before (left) and during (right) application of SKF 89976A. (F) Sample traces showing sIPSCs under control conditions (left) and in the presence of SNAP 5114 (10 μ_M) (right). (G–I) The cumulative distribution of the amplitude, inter-event interval and half-decay time of sIPSCs obtained from same neuron as in F. SNAP 5114 significantly shifts the amplitude distribution curve to the right (G) and inter-event interval distribution curve to the left (H) ($P = 0.001$), but has no significant effect on the distribution of sIPSC half-decay time (I) ($P = 0.08$). (J) Amplitude distribution histograms of sIPSCs recorded before (left) and during (right) application of SNAP 5114.

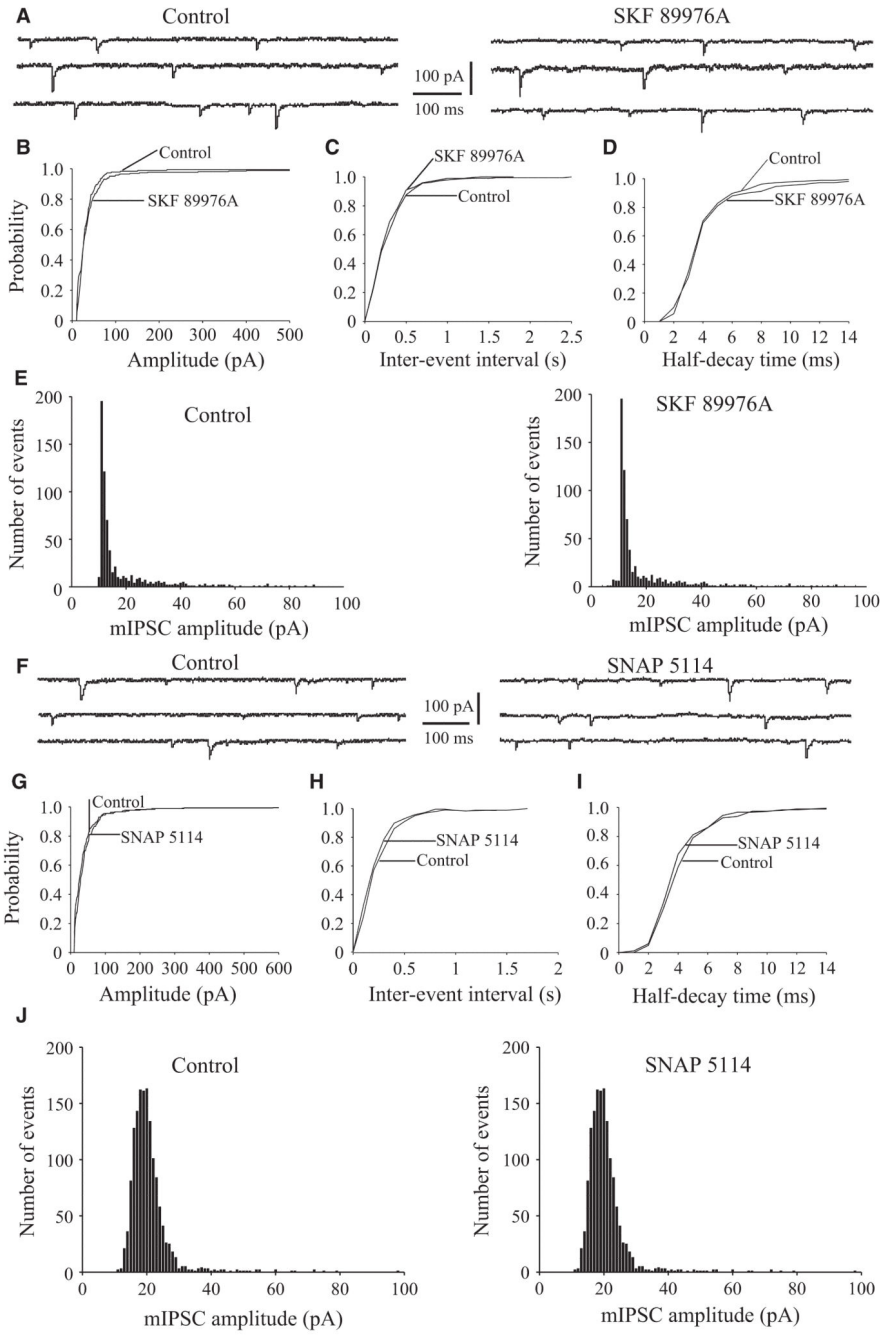

Fig. 6.

Effects of GAT-1 or GAT-3 applied alone or in combination on mIPSCs in rat GP neurons. (A) Sample traces showing mIPSCs recorded in GP neurons under control conditions (left) or during bath application of SKF 89976A (10 μ_M) (right). These mIPSCs were recorded in the presence of 50 μ_M CNQX, 50 μ_M D-AP5 and 1 μ_M TTX. (B–D) The cumulative distribution of the amplitude, inter-event interval and half-decay time of mIPSCs obtained from the same neuron as in A. SKF 89976A has no significant effect ($P = 0.07$) on the amplitude (left), inter-event interval (middle) or half-decay time (right) distribution curves

of mIPSCs. (E) Amplitude distribution histograms of mIPSCs recorded before (left) and during (right) application of SKF 89976A. (F) Sample traces showing mIPSCs recorded in rat GP neurons under control conditions (left) or during bath application of SNAP 5114 (10 μ_M) (right). (G–I) The cumulative distribution of the amplitude, interevent interval and half-decay time of mIPSCs recorded from the same neuron as in F. SNAP 5114 has no significant effect ($P = 0.06$) on the amplitude (left), interevent interval (middle) or half-decay time (right) distribution curves of mIPSCs. (J) Amplitude distribution histograms of mIPSCs recorded before (left) and during (right) application of SNAP 5114.

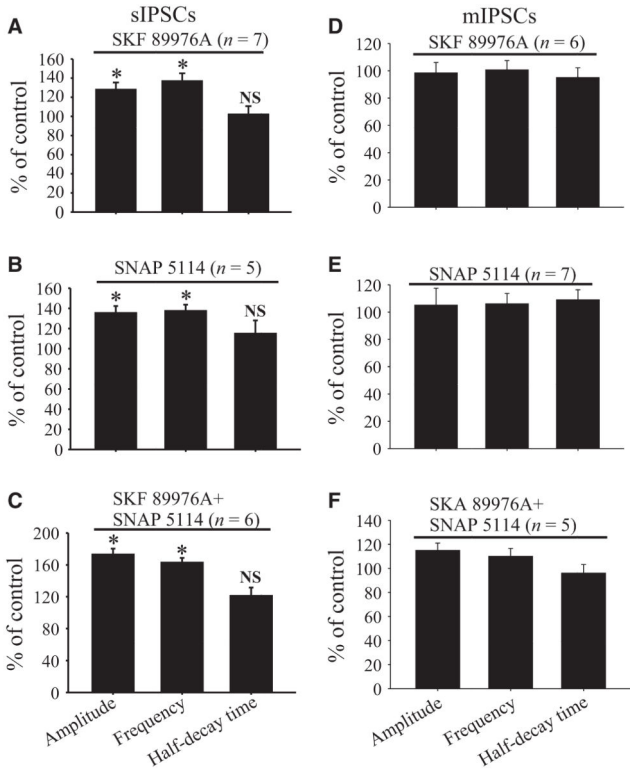

Fig. 7.

Summary bar graphs showing effects of SKF 89976A (A and D), SNAP 5114 (B and E) and SKF 89976A together with SNAP 5114 (C and F) application on the amplitude, frequency and half-decay time expressed as percentage of control ± SEM of sIPSCs (A–C) or mIPSCs (D–F) in the rat GP. (*Significant differences from control conditions, $P = 0.001$.)

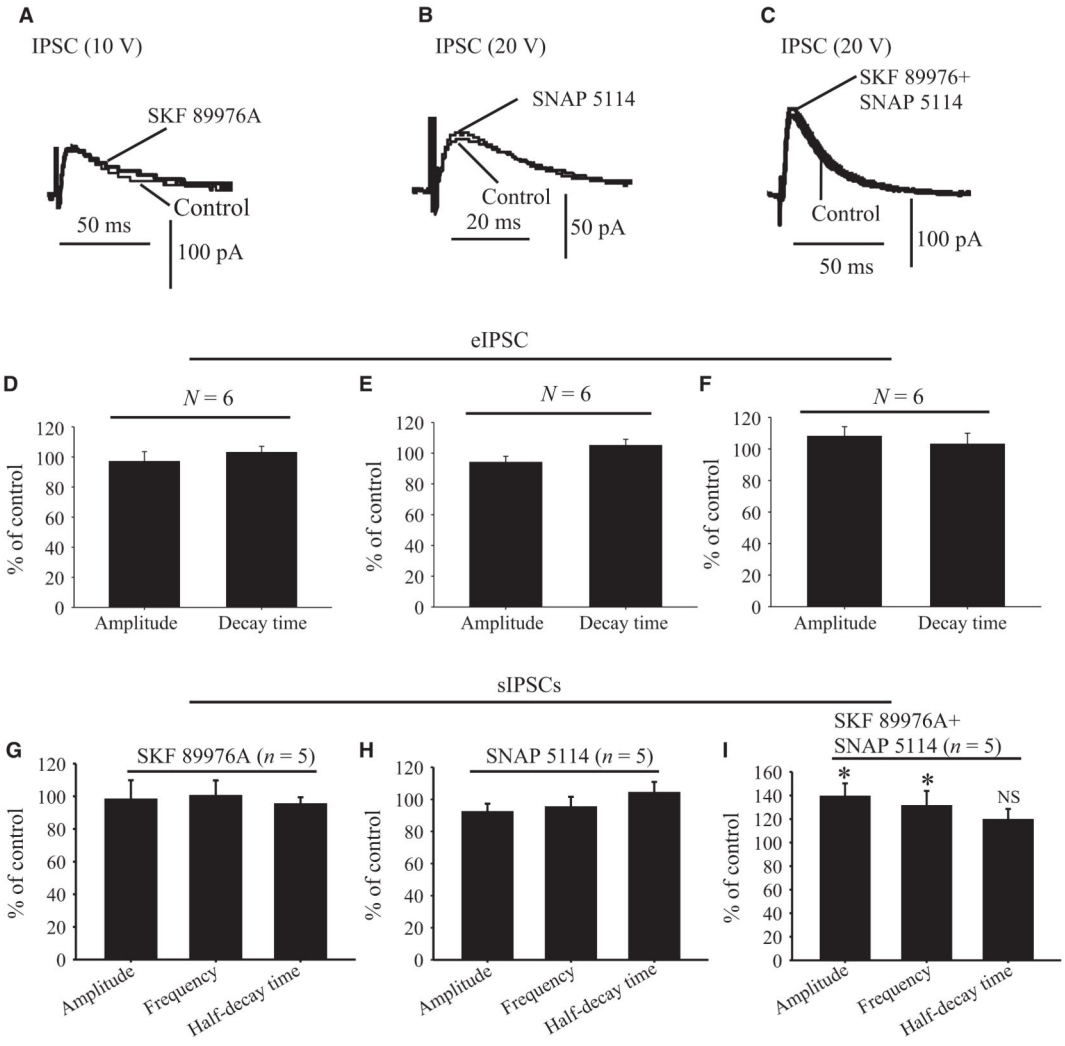

Fig. 8.

Effects of GAT-1, GAT-3 or GAT-1 combined with GAT-3 inhibitors on IPSCs evoked in GP neurons by local intrapallidal stimulation in coronal striatopallidal slice preparations. Application of SKF 89976A (A), SNAP 5114 (B) or SKF 89976A together with SNAP 5114 (C) has no significant effect on the amplitude and decay time of IPSCs evoked in GP neurons by local intrapallidal stimulation (20 V) in coronal slices of rat striatopallidal complex. (D–F) Summary bar graphs showing that the amplitude and decay time of eIPSCs in the rat GP are not changed in the presence of SKF 89976A (D), SNAP 5114 (E) or SKF 89976A together with SNAP 5114 (F) expressed as percentage of control ± SEM ($P = 0.06$). (G–I) Summary bar graphs showing that the amplitude, frequency and half-decay time of sIPSCs are not altered in presence of SKF 89976A (G) or SNAP 5114 (H) alone, but that their amplitude and frequency are significantly increased in the presence of SKF 89976A together with SNAP 5114, expressed as percentage of control ± SEM (*$P = 0.001$) (I). *N*, number of cells tested; NS, not significant.

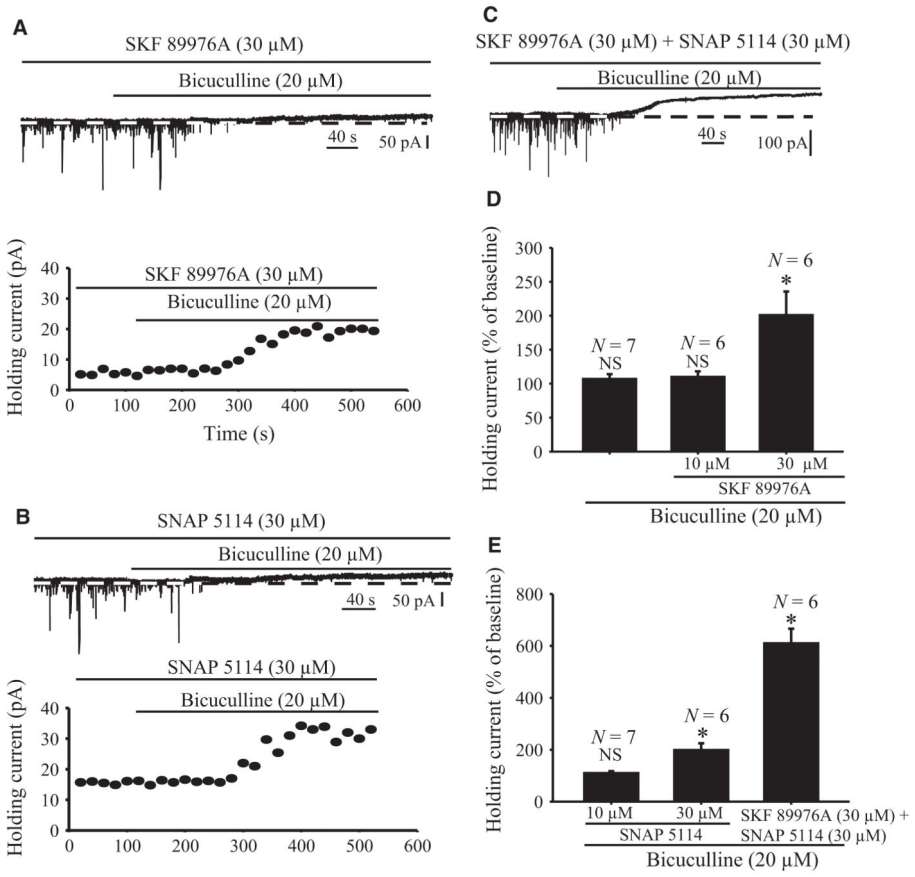

Fig. 9.

Application of GAT-1, GAT-3 or GAT-1 together with GAT-3 inhibitors induces $GABA_A$ receptor-mediated tonic currents in rat GP neurons. (A) Sample trace illustrates that application of bicuculline (20 μ_M) induces a tonic outward current in the presence of 30 μ_M SKF 89976A (top). Note that the sIPSCs are completely abolished by bicuculline in the presence of ionotropic glutamate receptor antagonists, confirming that they are mediated by $GABA_A$ receptor activation. The bottom graph shows the time course of bicuculline-induced tonic currents in the presence of 30 μ_M SKF 89976A in the neuron displayed in the top trace. (B) Sample trace showing that application of bicuculline (20 μ_M) induces tonic outward current (top). The bottom panel displays the time course of this current in the presence of 30 μ_M SNAP 5114. (C) Sample trace showing that bicuculline induces tonic current in the presence of 30 μ_M SKF 89976A together with 30 μ_M SNAP 5114. (D–E) Summary bar graphs showing the effects of bicuculline alone, or together with SKF 89976A (10 and 30 μ_M) (top graph), SNAP 5114 (10 and 30 μ_M) or SKF 89976A plus SNAP 5114 (bottom), on holding current expressed as percentage of control. (*Significant difference from control, $P = 0.001$.) *N*, number of cells tested; NS, not significant.